NANO LETTERS

Letter

Bulk Production of a New Form of sp Carbon: Crystalline Graphene Nanoribbons

Jessica Campos-Delgado, Jose# Manuel Romo-Herrera, Xiaoting Jia, David A. Cullen, Hiroyuki Muramatsu, Yoong Ahm Kim, Takuya Hayashi, Zhifeng Ren, David J. Smith, Yu Okuno, Tomonori Ohba, Hirofumi Kanoh, Katsumi Kaneko, Morinobu Endo, Humberto Terrones, Mildred S. Dresselhaus, and Mauricio Terrones

Nano Lett., **2008**, 8 (9), 2773-2778• DOI: 10.1021/nl801316d • Publication Date (Web): 14 August 2008

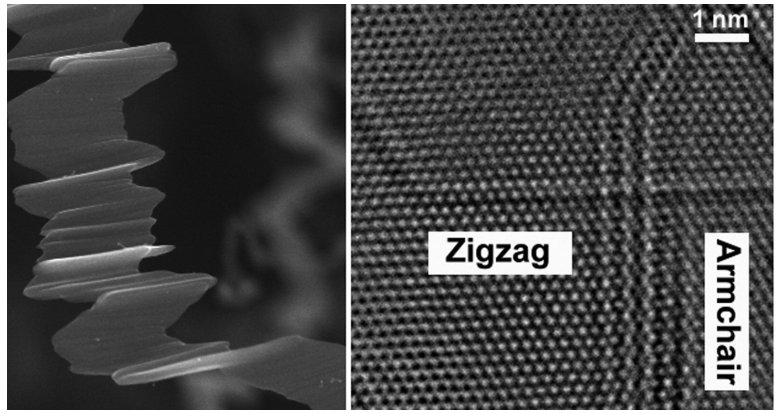

More About This Article

Additional resources and features associated with this article are available within the HTML version:

- Supporting Information
- Links to the 1 articles that cite this article, as of the time of this article download
- Access to high resolution figures
- Links to articles and content related to this article
- Copyright permission to reproduce figures and/or text from this article

View the Full Text HTML

Nano Letters is published by the American Chemical Society. 1155 Sixteenth Street N.W., Washington, DC 20036

NANO LETTERS

2008
Vol. 8, No. 9
2773-2778

Bulk Production of a New Form of sp^2 Carbon: Crystalline Graphene Nanoribbons

Jessica Campos-Delgado,[†] José Manuel Romo-Herrera,[†] Xiaoting Jia,[‡] David A. Cullen,[§] Hiroyuki Muramatsu,[||] Yoong Ahm Kim,[||] Takuya Hayashi,[||] Zhifeng Ren,[⊥] David J. Smith,[§] Yu Okuno,[#] Tomonori Ohba,[#] Hirofumi Kanoh,[#] Katsumi Kaneko,[#] Morinobu Endo,[||] Humberto Terrones,[†] Mildred S. Dresselhaus,[&] and Mauricio Terrones*[,†]

Advanced Materials Department, IPICYT, Camino a la Presa San José 2055, Col. Lomas 4a. sección, San Luis Potosí 78216, México, Department of Materials Science and Engineering, Massachusetts Institute of Technology, Cambridge, Massachusetts 02139-4307, School of Materials and Department of Physics, Arizona State University, Tempe Arizona 85287-1504, Faculty of Engineering, Shinshu University, 4-17-1 Wakasato, Nagano-shi 380-8553, Japan, Department of Physics, Boston College, Chestnut Hill, Massachusetts 02467, Molecular Chemistry Group, Department of Chemistry, Faculty of Science, Chiba University, 1-33 Yayoi, Inage-ku, Chiba-shi 263-8522, Japan, and Department of Electrical Engineering and Computer Science and Department of Physics, Massachusetts Institute of Technology, Cambridge, Massachusetts 02139-4307

Received May 8, 2008; Revised Manuscript Received July 10, 2008

ABSTRACT

We report the use of chemical vapor deposition (CVD) for the bulk production (grams per day) of long, thin, and highly crystalline graphene ribbons (<20−30 μm in length) exhibiting widths of 20−300 nm and small thicknesses (2−40 layers). These layers usually exhibit perfect ABAB... stacking as in graphite crystals. The structure of the ribbons has been carefully characterized by several techniques and the electronic transport and gas adsorption properties have been measured. With this material available to researchers, it should be possible to develop new applications and physicochemical phenomena associated with layered graphene.

Following the discovery of C_{60}[1] and its bulk production,[2] nanoscale carbon science emerged, and other fullerene-like carbons, such as nanotubes,[3−5] started to attract the attention of numerous researchers because of their fascinating physicochemical properties. Subsequently, different experimental approaches have led to the synthesis of graphitic nanocones and nanodiscs,[6] as well as nanohorns[7] and toroidal structures.[8,9] These results have also motivated theoretical studies on novel forms of carbon such as Schwartzites, toroids, fullerenes, nanotubes, and graphene nanoribbons. In particular, graphene ribbons have been predicted to be metallic if their edges exhibit a zigzag morphology, whereas armchair edges can give rise to either semiconducting or metallic transport.[10] This theoretical work has motivated the synthesis of individual graphene sheets and nanoribbons.

It has been shown experimentally that zigzag and armchair graphene ribbon edges result in different Raman spectra[11] and electronic properties.[12] For example, armchair edges result in a large intensity Raman D band, whereas the D-band signal from zigzag edges is substantially reduced.[11] In addition, the zigzag edges appear to have a high density of electronic states at the Fermi level.[10] Experimental investigations are now directed toward synthesizing individual graphene sheets in order to characterize Raman modes as well as physicochemical properties.[12−22] With these techniques, substrates (highly oriented pyrolytic graphite-HOPG) are used as a source of individual sheets. Unfortunately,

* To whom correspondence should be addressed. Fax: +52(444) 834-2010. E-mail: mterrones@ipicyt.edu.mx.
[†] Advanced Materials Department IPICYT.
[‡] Department of Materials Science and Engineering, Massachusetts Institute of Technology.
[§] Arizona State University.
[||] Shinshu University.
[⊥] Boston College.
[#] Chiba University.
[&] Department of Electrical Engineering and Computer Science and Department of Physics, Massachusetts Institute of Technology.

10.1021/nl801316d CCC: $40.75
Published on Web 08/14/2008

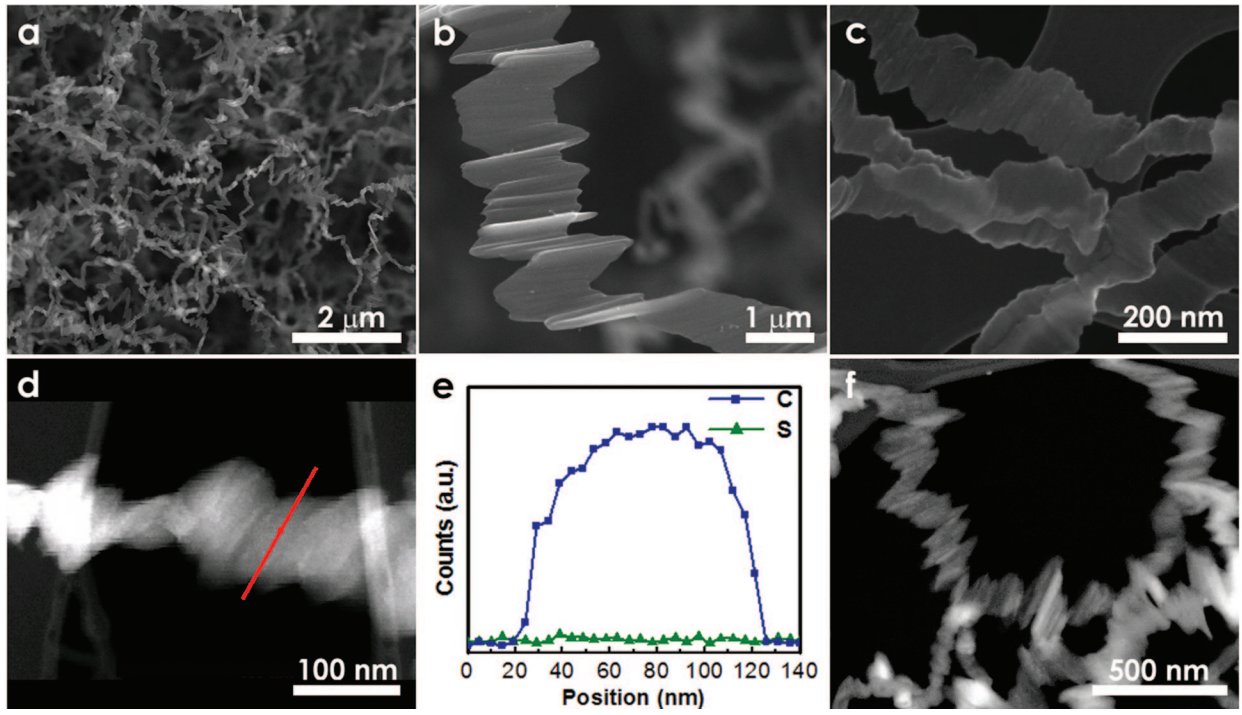

Figure 1. (a−c) SEM images of graphene nanoribbons at different magnification. Note that the ribbons are very thin (<10 nm) and could be transparent to the SEM beam (see c); (d) HAADF image of a nanoribbon and its corresponding elemental EDX line-scan, indicated by the line. The elemental profile (e) shows the absence of S and indicates that the ribbon mainly consists of C; (f) dark field STEM image of bulk nanoribbons displaying rippled regions within the ribbons.

current synthesis methods make difficult the manipulation of the nanoribbons, and the amount of available sheet material is very limited for use in applications. However and to the best of our knowledge, the bulk synthesis of layered graphene ribbons has not been reported hitherto. In this account, we report the use of chemical vapor deposition (CVD) for one-step production of bulk quantities of thin graphite ribbons. This material has been carefully characterized by several techniques as summarized below.

The synthesis of these graphite nanoribbons was carried out using the aerosol pyrolysis process.[23] Solutions containing 2.80 g of ferrocene ($FeCp_2$) and 0.266 mL of thiophene (C_4H_4S) in 280 mL of ethanol (CH_3CH_2OH) were used. An aerosol was generated ultrasonically and then carried by an argon flow (0.8 L/min) into a quartz tube located inside a two-furnace system heated to 1223 K (both furnaces were operated at the same temperature). After 30 min of operation, the ultrasonic sprayer was turned off, the Ar flow was decreased to 0.2−0.3 L/min, and the furnaces were allowed to cool to room temperature. Once the system had cooled down, the quartz tube was removed and a black powder material was scraped from the walls of the tube located in the first furnace area.

The morphology, structural, and other physicochemical properties were extensively studied by SEM (FEI-field emission SEM - XL30 operated at 1−15 keV), HRTEM (JEOL JEM-2010 FEF instrument operated at 200 kV, JEOL JEM 4000EX operated at 400 kV, JEOL JEM-2010F operated at 200 kV and equipped with a thin-window light-element-sensitive X-ray detector, a Gatan Enfina EELS instrument for high spatial resolution microanalysis, and a Philips CM20 operated at 200 kV), TGA (Thermo Haake, Cahn VersaTherm HS heating at 5 K/min to 1173 K in air), XRD (Brucker D8-advanced equipped with a Cu anode (λ = 1.5406 Å) operated at 35 kV, 25 mA, and 293 K), Raman spectroscopy (a Renishaw system equipped with laser excitation line λ = 514 nm (2.41 eV)), and X-ray photoelectron spectroscopy (XPS; JEOL; JPS-9010MX using Mg Kα radiation at 10^{-6} Pa, XPS spectrum being deconvoluted with a Gaussian−Lorentzian mixed function after correction). Adsorption isotherms of N_2 and H_2 were measured volumetrically at 77 K after preheating in vacuo.

We also carried out transport measurements on individual nanoribbons inside the HRTEM and performed Joule heating experiments that resulted in the generation of highly crystalline graphite nanoribbons. This was achieved using a HRTEM (JEOL 2010F operated at 200 KeV) equipped with a scanning tunnelling microscope (STM) probe, attached to a piezoelectric stage. In particular, each nanoribbon in the HRTEM was attached to two electrodes. Subsequently, a voltage was applied across the nanoribbon and the changes in the current and morphology were monitored in real time.

The morphology of the initial black powder consisted of ribbon-like structures exhibiting lengths of several micrometers, widths ranging from 20 to 300 nm and thicknesses of <15 nm (Figure 1). It is interesting to note that the initial ribbons revealed both flat regions and rippled areas (Figure 1b). The edges of the as-prepared ribbons also displayed relatively sharp cuts that could be related to the presence of either zigzag or armchair edges (Figure 1b,c). Since the ribbons were extremely thin, SEM images almost suggested transparency when observed at 10−15 keV; note the presence

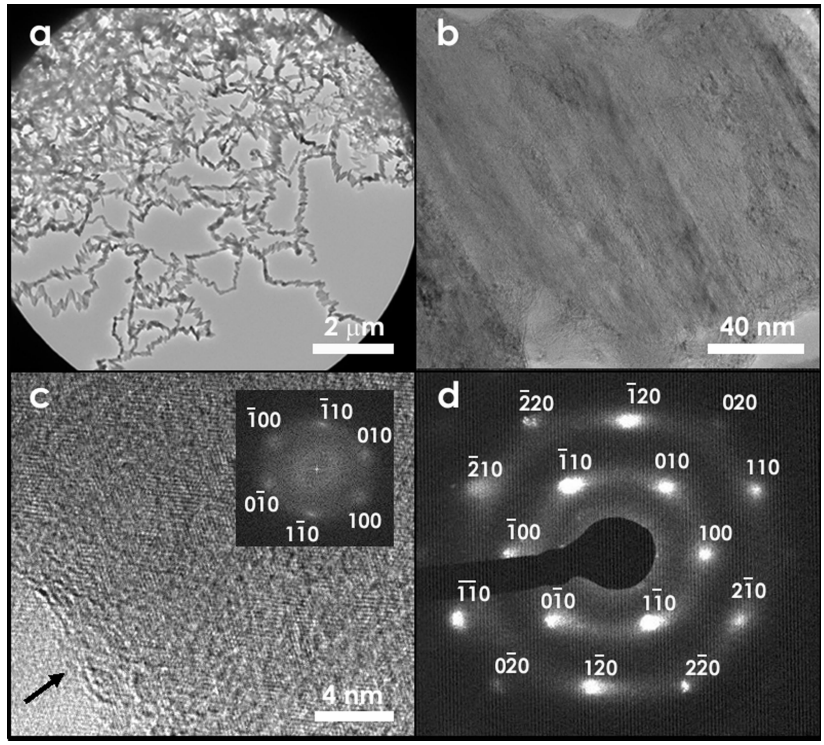

Figure 2. (a,b) Low and high magnification TEM images of graphene nanoribbons; (c) HRTEM image of a ribbon edge (the arrow indicates the ribbon edge) displaying a hexagonal pattern, and its corresponding FFT (inset); (d) indexed electron diffraction pattern of an individual thin graphene nanoribbon (ca. 10 nm thick) showing the ABAB... stacking of the graphite structure with a 3D order.

of the holey carbon grid underneath the ribbons in Figure 1c.

High-angle annular-dark-field (HAADF), using scanning transmission electron microscopy (STEM), and dark-field images of the ribbons are depicted in Figure 1d,f, respectively. The ribbons displayed only one type of contrast, and Fe catalyst particles were never observed in these structures (note that carbon nanotubes containing metal catalyst particles at the nanotube tips were usually produced in the second furnace while the graphene nanoribbon material was extracted from the first furnace). By performing detailed elemental energy dispersive X-ray (EDX) spectroscopy linescans along the ribbon surface (Figure 1e), it was found that the nanoribbons consisted of C, while S was notably absent. Even surface-sensitive XPS could not detect any trace of S. Although graphene nanoribbons consist of only carbon, S appears to be crucial for growing the ribbons, and it could well act as a catalyst. It is also important to emphasize that only minute amounts of S are sufficient and necessary to grow the ribbons, and an excess of S results in the complete inhibition of ribbon formation. We believe that Fe helps to create the conditions to crack the molecules (ethanol and thiophene) so that S and C interact somehow to grow the ribbons.

In order to carry out TEM and HRTEM studies, the ribbon material (2−5 mg) was dispersed ultrasonically in methanol (10 mL) and deposited on holey carbon grids. Figure 2 depicts ribbons under TEM and HRTEM imaging conditions. At low magnification, the material consisted only of carbon ribbons (Figure 2a). HRTEM images of the ribbons (Figure 2b,c) revealed the presence of hexagonal patterns, which were confirmed after obtaining the fast Fourier transform (FFT; see Figure 2c inset). In order to study the graphitic structure and layer stacking and to identify the edge structure, electron diffraction patterns were recorded from different ribbons (Figure 2d). Interestingly, all of the analyzed ribbons consisted of ABAB... stacked graphite (since all reflections from three-dimensional, 3D, graphite are visible in Figure 2d), and the edges exhibited armchair and zigzag (or close to zigzag) morphologies (see below).

The average bulk structure of the pristine ribbon material was further studied by XRD. It was found that the nanoribbons exhibited a highly crystalline graphite-like structure, with the presence of strong (002), (100), (101), (004), and (110) reflections (Figure 3a). Moreover, the line width of the (002) diffraction line gave an average L_c crystallite size of approximately 10−14 nm, in good agreement with SEM observations.

The reproducibility of the experiments was confirmed. Nevertheless, some variables were critical. One was the storage time of the solution. We found that, 3 weeks after preparation, the quality of the resulting thin graphene ribbon material deteriorated relative to that obtained with a fresh solution and that more byproduct was produced (short nanotubes in addition to iron particles).

Bulk Raman spectroscopy measurements on the ribbons revealed the presence of the D and G bands, located at 1355 and 1584 cm^{-1}, respectively (Figure 3b). In general, it was found that the D band exhibited the highest intensity, probably because of the high proportion of edges and ripples within the ribbons. Other defect-sensitive Raman features were also intense. In particular, we noted that, when we

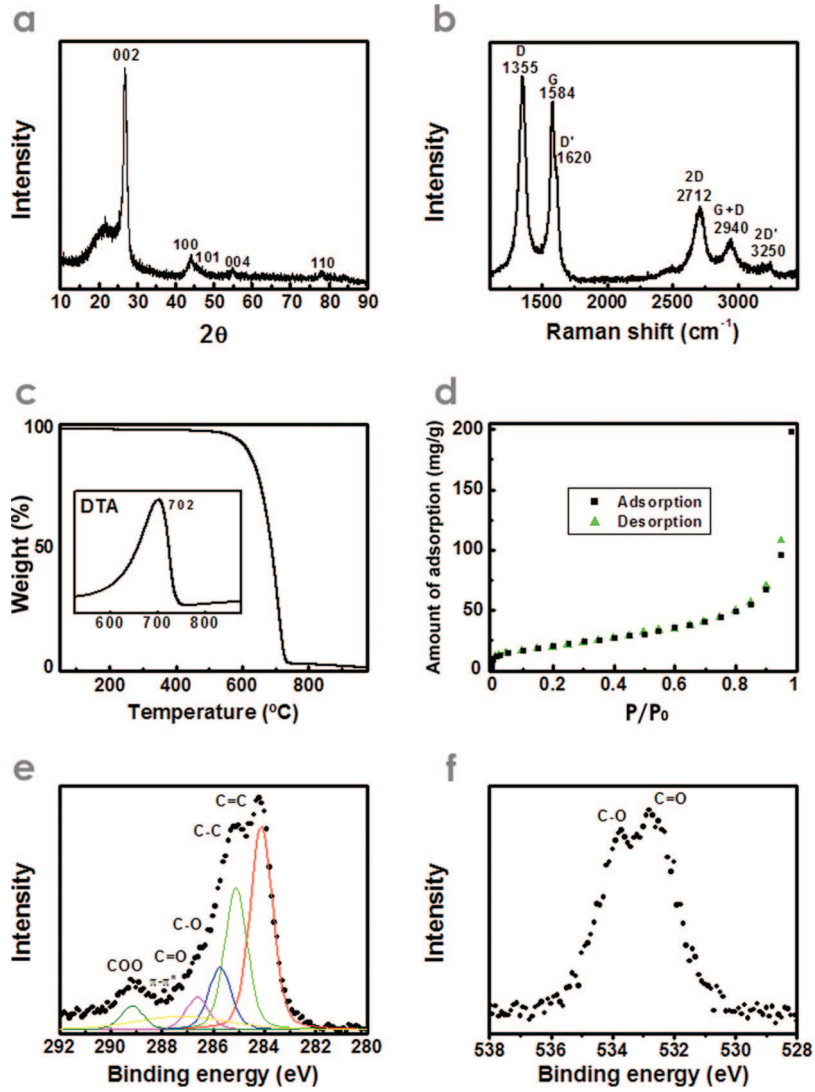

Figure 3. (a) XRD pattern of a bulk nanoribbon sample; (b) typical Raman spectrum of bulk nanoribbons showing the presence of the D and G band as well as the overtone and combination mode features taken at 514 nm laser excitation; (c) TGA plot and its first derivative presented in the inset showing the behavior of the DTA peak in an oxygen atmosphere for the ribbon material at high temperature; (d) A Typical N_2 adsorption isotherm of the nanoribbon sample; (e) XPS data of graphene nanoribbons for the C binding energies; it is clear that sp^2 and sp^3 hybridized carbon atoms are included in the sample with a 1:1 ratio, as well as carbonyl groups (C═O) and carboxylic groups (COO); and (f) XPS data for graphene nanoribbon material corresponding to the O binding energies, confirming the presence of different O terminated edges.

recorded Raman spectra from individual ribbon edges, the presence of the D′ feature at 1620 cm^{-1} was especially pronounced and well-defined and identified with the large number of ribbon edge structures (results not shown here). The disorder-induced combination mode (D + G) at about 2940 cm^{-1} is also exceptionally strong. Further Raman analyses on individual ribbons are currently underway, since new structural features were identified on individual ribbons.

In order to confirm that the nanoribbons were highly crystalline, we performed TGA studies. It was found that the decomposition temperature of the ribbons in air corresponded to 702 °C (Figure 3c). This value is almost the same as that observed in highly crystalline carbon nanotubes produced by arc discharge techniques.[24]

Nitrogen (N_2) adsorption measurements on the carbon nanoribbons (Figure 3d) revealed a BET surface area of 59 m^2/g, which was similar to the surface area of acetylene black (86 m^2/g). The adsorption data indicated that the nanoribbon material corresponds to a flat surface, which was not porous to N_2 molecules. The interaction of a N_2 molecule with the surface of the nanoribbon is weaker than that with highly crystalline carbon black, which is in agreement with the presence of predominant edge-like surfaces. However, H_2 adsorption at 77 K indicated the presence of rather strong sites for supercritical H_2 adsorption corresponding to approximately 15% of the monolayer capacity of N_2. Consequently, the nanoribbon should have a unique nanostructural fit for the adsorption of supercritical H_2.

XPS studies revealed the nature of the carbon bonds present in the sample (Figure 3e,f). The material contained sp^2 and sp^3 hybridized carbon atoms (39% sp^2 and 39% sp^3; Figure 3e), and the rest of the carbonaceous material was bonded to O (Figure 3f) and consisted of carbonyl groups (C═O) and carboxylic groups (COO); note that 85 atom %

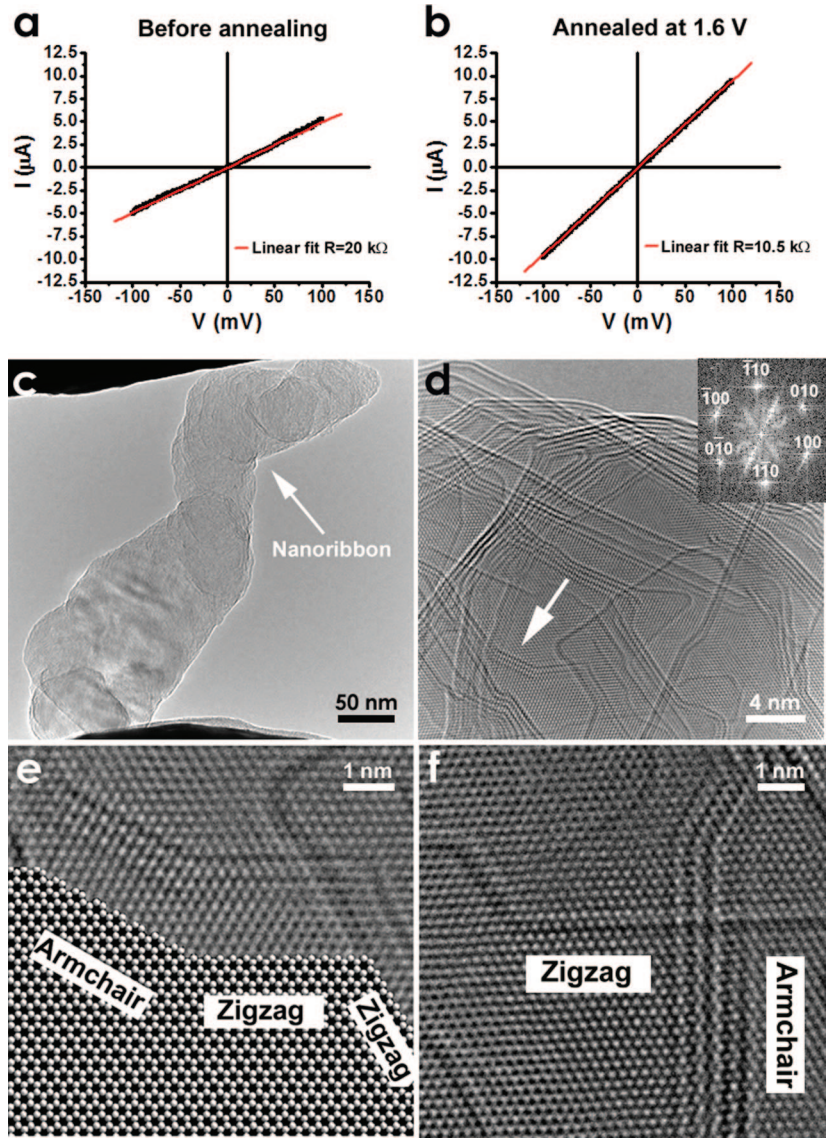

Figure 4. (a,b) Characteristic $I-V$ curves of graphene nanoribbons, before annealing and after annealing when subjected to 1.6 V. The measurements were performed inside an HRTEM equipped with a piezo stage that enabled contact between the ribbons with two electrodes; (c) TEM image of the ribbon in (a) which was adhered to the two electrodes; (d) HRTEM image of the ribbon shown in (c) after annealing using a voltage of 1.6 V. The image depicts multiple graphene layers of the ribbon and reveals a perfect hexagonal pattern (see FFT inset), which is commensurate with the crystalline structure of ABAB; (e,f) HRTEM image of the region indicated with the arrow in (d) clearly showing the presence of zigzag and armchair edges, and (f) HRTEM image of another region of the Joule heated ribbon showing the presence of armchair and zigzag edges. Note that the lower part of (e) is a schematic diagram of the hexagonal structure seen in the HRTEM image.

corresponded to C and 15 atom % to O. We believe that the large number of sp^3 hybridized carbon atoms was caused by the exposed edges and the rippled (highly curved) regions within the nanoribbons. The 1:1 ratio of sp^3/sp^2 carbon atoms could also explain the large intensity of the D band observed in Raman spectroscopy, because the material was indeed highly crystalline and showed an AB... stacking of the graphene layers.

We also carried out electron energy loss spectroscopy (EELS) studies on different ribbons. However, we could not conclude clear changes between the different regions of the ribbons since the results were very variable because of the rippled areas of the ribbons' interior also exhibited sp^3 hybridized carbon. If the ribbons would be completely flat, this ratio would have been easier to calculate. In some cases, we observed the sp^3/sp^2 ratio close to 1:1, but in other areas, we observed the domination of the sp^2 hybridized carbon (see Supporting Information Figure S1). Therefore, further and detailed EELS studies are still required because it is likely that armchair and zigzag edges would exhibit different features.

In order to study electron transport along these nanoribbons, we carried out in situ transport measurements using a piezo stage inside a HRTEM (Figure 4). Two electrodes were attached to a piece of an individual ribbon, and a voltage was applied across the ribbon (Figure 4c). Subsequently, $I-V$ curves for different ribbons were obtained (see Figure 4a,b). For all ribbons studied, the material behaved like a metal

(straight line for the $I-V$ curves) that followed Ohm's law. For the ribbon shown in Figure 4c, a 20 kΩ resistance value was measured when a low voltage was applied. Interestingly, after a voltage of 1.6 V was applied for more than 15 min, the resistance value dropped to 10.5 kΩ, corresponding to the structure shown in Figure 4d, suggesting that crystallization of the material due to Joule heating had taken place. These results (Figure 4a,b) confirm that the ribbons behave like metals. Specifically, Figure 4e,f reveals the exceptional clarity of the many long zigzag and armchair edges that are usually observed after the Joule heating is applied, based on the angles between adjacent edges and the atomic orientations. In addition, the FFT from Figure 4e,f (shown as an inset to Figure 4d) confirms the AB layer stacking of the graphene ribbon. Further studies of the edges of these graphene ribbons are in progress.

We identify the mechanism responsible for the observed increase in crystallinity with an electro-migration process which serves to anneal defects. Beyond some specific value of the applied voltage, the temperature of the ribbon gets too high which combined with long-term (>15 min) exposure to beam irradiation causes breakdown of the graphene layers.

Because of their highly crystalline layered structure, these ribbons could also be exfoliated (detachment of the layers into individual layers) and cut into shorter pieces. The exfoliation process usually consists of intercalating atoms or molecules (e.g., Li, K, H_2SO_4, $FeCl_3$, Br_2, etc.) between layers, followed by rapid reactions in liquids or by subjecting the material to abrupt temperature changes. It is clear that the exfoliated form of these ribbons (containing several exposed edges) could be used as gas storage devices, electronic wires, sensors, catalytic substrates, field emission sources, batteries, and so forth. By using this material, it is now possible to unveil new applications and novel physicochemical properties associated with layered carbon.

It is important to emphasize that a single-step CVD process was used here to synthesize the nanoribbons under atmospheric pressure conditions, at relatively high temperature (1223 K). Furthermore, the physicochemical properties of these ribbons are novel when compared with other forms of carbon.

In summary, we have shown here that it is possible to synthesize bulk amounts of a novel form of nanocarbon (graphene nanoribbons). This material was characterized using diverse techniques and the results have confirmed that graphene nanoribbons are indeed a promising novel form of carbon which could be interesting for both scientific studies of graphene edges and for practical applications because of the availability of large quantities of ribbons. It is possible that these ribbons could be exfoliated into individual graphene sheets providing new possibilities in the future for detailed studies of the structure and properties of clean graphene edges, not previously available.

Acknowledgment. This work was sponsored by CONACYT-Mexico Grants 56787 (Laboratory for Nanoscience and Nanotechnology Research-LINAN), 45762 (H.T.), 45772 (M.T.), 41464-Inter American Collaboration (M.T.), 42428-Inter American Collaboration (H.T.), 2004−01−013/SALUD-CONACYT (M.T.), and Ph.D. Scholarship (J.C.-D., J.M.R.-H.). We also thank the MIT-CONACYT grant on doped nanocarbons for financial support (M.S.D., M.T.), NSF/CTS-05−06830 (M.S.D. and Z.R.) and NSF Grant DMR-03−03429 (D.J.S.). M.E. thanks Grant-in-Aid for Specially Promoted Research (No. 19002007) of Ministry of Education, Culture, Sports, Science and Technology of Japan. K.K. thanks Grant-in-Aids for Scientific Research S(15101003) from the Japanese Government. Authors are grateful to I. Maciel, A. Jorio, M. Pimenta, A. Botello, F. López-Urias, D. Ramírez, G. Ramírez, and G. Pérez Assaf for fruitful discussions.

Supporting Information Available: EELS spectra. This material is available free of charge via the Internet at http://pubs.acs.org.

References

(1) Kroto, H. W.; Heath, J. R.; O'Brien, S. C.; Curl, R. F.; Smalley, R. E. *Nature* **1985**, *318*, 162–163.
(2) Krätschmer, W.; Lamb, L. D.; Fostiropoulos, K.; Huffman, D. R. *Nature* **1990**, *347*, 354–358.
(3) Oberlin, A.; Endo, M.; Koyama, T. *J. Cryst. Growth* **1976**, *32*, 335–349.
(4) Ebbesen, T. W.; Ajayan, P. M. *Nature* **1992**, *358*, 220–221.
(5) Iijima, S. *Nature* **1991**, *354*, 56–58.
(6) Krishnan, A. et al. *Nature* **1997**, *388*, 451–454.
(7) Iijima, S.; Yudasaka, M.; Yamada, R.; Bandow, S.; Suenaga, K.; Kokai, F.; Takahashi, K. *Chem. Phys. Lett.* **1999**, *309*, 165–170.
(8) Liu, J.; Dai, H.; Hafner, J. H.; Colbert, D. T.; Smalley, R. E.; Tans, S. J.; Dekker, C. *Nature* **1997**, *385*, 780–781.
(9) Martel, R.; Shea, H. R.; Avouris, P. *Nature* **1999**, *398*, 299–299.
(10) Nakada, K.; Fujita, M.; Dresselhaus, G.; Dresselhaus, M. S. *Phys. Rev. B* **1996**, *54*, 24.
(11) Cançado, L. G.; Pimenta, M. A.; Neves, B. R. A.; Medeiros-Ribeiro, G.; Enoki, T.; Kobayashi, Y.; Takai, K.; Fukui, K.; Dresselhaus, M. S.; Saito, R.; Jorio, A. *Phys. Rev. Lett.* **2004**, *93* (4), 047403.
(12) Kobayashi, Y.; Fukui, K.; Enoki, T.; Kusakabe, K.; Kaburagi, Y. *Phys. Rev. B* 2005, *71*, 193406−1−4.
(13) Affoune, A. M.; Prasad, B. L. V.; Sato, H.; Enoki, T.; Kaburagi, Y.; Hisiyama, Y. *Chem. Phys. Lett.* **2001**, *348*, 17.
(14) Novoselov, K. S.; Jiang, D.; Schedin, F.; Booth, T. J.; Khotkevich, V. V.; Morozov, S. V.; Geim, A. K. *PNAS* **2005**, *102*, 10451–10453.
(15) Berger, C.; Song, Z.; Li, T.; Li, X.; Ogbazghi, A. Y.; Feng, R.; Dai, Z.; Marchenkov, A. N.; Conrad, E. H.; First, P. N.; de Heer, W. A. *J. Phys. Chem. B* **2004**, *108*, 19912.
(16) Hass, J.; et al. *Appl. Phys. Lett.* **2006**, *89*, 143106.
(17) Charrier, A.; Coati, A.; Argunova, T. *J. Appl. Phys.* **2002**, *92*, 2479.
(18) Forbeaux, I.; Themlin, J. M.; Debever, J. M. *Phys. Rev. B* **1998**, *58*, 16396.
(19) Ferrari, A. C.; Meyer, J. C.; Scardaci, V.; Casiraghi, C.; Lazzeri, M.; Mauri, F.; Piscanec, S.; Jian, D.; Novoselov, K. S.; Roth, S.; Geim, A. K. *Phys. Rev. Lett.* **2006**, *97*, 187401.
(20) Gupta, A.; Chen, G.; Joshi, P.; Tadigadapa, S.; Eklund, P. C. *Nano Lett.* **2006**, *6*, 2667.
(21) Malard, L. M.; Nilsson, J.; Elias, D. C.; Brant, J. C.; Plentz, F.; Alves, E. S.; Castro Neto, A. H.; Pimenta, M. A. *Phys. Rev. B* 2007, *76*, 201401 (R).
(22) Faugeras, C.; Nerrière, A.; Potemski, M.; Mahmood, A.; Dujardin, E.; Berger, C.; de Heer, W. A. *Appl. Phys. Lett.* **2008**, *92*, 011914.
(23) Pinault, M.; Mayne-L'Hermite, H.; Reynaud, C.; Beyssac, O.; Rouzaud, J. N.; Clinard, C. *Diamond Relat. Mater.* **2004**, *13*, 1266–1269.
(24) Terrones, M.; Hsu, W. K.; Kroto, H. W.; Walton, D. R. M. In Fullerenes and Related Structures; Editor, Hirsch, A. *Topics in Chemistry Series*; Springer-Verlag: Berlin, 1999; Vol. 199, pp 189−234.

NL801316D